A Computational Analysis of Unsteady Transonic/Supersonic Flows Over Backward Facing Step in Air Jet Nozzle

Sang Dug Kim
School of Automotive, Industrial, Mechanical Engineering, Daegu University, Gyongsan 712-714, Korea
Jeong Ill Seo
Agency of Defense Development, Daejeon 305-152, Korea
Dong Joo Song*
School of Mechanical Engineering, Yeungnam University, Gyongsan 712-749, Korea

A transonic/supersonic axisymmetric backward facing step nozzle flow in an air-jet loom has been analyzed numerically by using a time accurate characteristic based upwind flux difference splitting compressible Navier-Stokes method. The unsteady pressure and Mach number behavior along the center line of the main nozzle were analyzed by periodic inlet condition changes to simulate the intermittent flow inside main nozzle of an air-jet loom.

Key Words : Transonic/Supersonic Flows, Air Jet Loom, Flux Difference Splitting Nethod, Backward facing Step, Unsteady Flow, Recirculating Flow

Nomenclature

C_L: Lift coefficient
C_p: Pressure coefficient
d : Inner diameter of needle
L : Acceleration tube length
M : Mach number
R : Residual, radius of acceleration tube
α : Angle of attack
ϕ : Time accuracy coefficient

1. Introduction

An air-jet loom inserts the weft into the warp by using high pressure air-jet thrust force and skin friction force along the yarn. Air-jet loom is popular in texturing industries because of its high productivity, convenient controllability, and wide variety of textured fabrics : silk, cotton, wool, and spun textures. Air-jet loom is also capable of texturing spun or cellulose filament fabrics, which cannot be woven by water-jet looms. However, since density of air is too low compared with that of water, compressed air jet diffuses rapidly into the atmosphere after discharging from acceleration tube. Also viscosity of air is about 1/50 of water viscosity, so air consumption becomes critical in air-jet loom. Due to large consumption of air, main nozzle shape, exit shape of subnozzle, subnozzle locations, and control methods have been studied intensively to reduce air consumption in air-jet looms.

Fundamental research in backward-facing step shape main nozzle is especially necessary to design optimum shapes of the main nozzles. Reduced air diffusion and effective control of flow direction and velocity are therefore very important in air-jet loom design. Due to recent development of high speed air-jet looms, analyses of transonic/supersonic flows in main nozzles have become important for performance enhancement

* Corresponding Author,
E-mail : djsong@yu.ac.kr
TEL : +82-53-810-2449; **FAX** : +82-53-810-4627
School of Mechanical Engineering, Yeungnam University, Gyongsan 712-749, Korea. (Manuscript **Received** July 18, 2006; **Revised** December 1, 2006)

of air-jets and optimum nozzle design. It is very difficult to measure the flow inside nozzle throat region experimentally because of its small cross-sectional area ; however, the most important flow phenomena, such as shock waves and flow separations, occur frequently inside this nozzle throat area. Therefore, a computational approach may be necessary. Air flow inside the air-jet loom main nozzle shows subsonic, transonic, and supersonic flow characteristics. There are some difficulties in computational analysis due to the complexity of the flow nature, i.e., turbulence and shock wave/boundary layer interaction.

Duxbury and Lord (1959) derived air-jet velocity distribution exposed to free atmosphere from the main nozzle. Lyubovitskii (1966) measured supersonic pulsed jet flow from the nozzle exit. Uno and Ishida (1986) experimentally measured air-jet velocity and weft flying distance using various acceleration tube prototypes. Mohamed and Salama (1986) studied the effects of diameter and length of acceleration tubes on flow velocity. Oh et al.(2001) studied transonic/supersonic flow in the main nozzle of an air-jet loom by using steady compressible Navier-Stokes method. They analyzed the effects of air tank pressure, acceleration tube length and nozzle shape. Flow physics including choking phenomena at the nozzle throat and/or at exit of the acceleration tube were very important in designing optimum nozzle shape.

In this study unsteady compressible Navier-Stokes equations are solved to study unsteady intermittent flows in time accurate manner. For the accurate treatment of unsteady term one frequently uses time explicit Runge-Kutta method (Jorgenson and Chima, 1989), which has the advantages of simple calculation due to elimination of iterative inner calculation ; however, it has time step limitation by severe Courant-Friedrichs-Lewis condition. Any method with implicit inner iteration has less limitation on time step size and can increase stability of solution with repetitive calculation. Chow and Pulliam (1984) introduced an implicit approximate factorization in computing unsteady compressible flow. The important problem in unsteady flow calculation is how to accelerate the solution convergence while advancing time step. To expedite the solution convergence and to obtain stable solution one can advance solution by using a local time stepping method with pseudo time inner iteration, or introducing residual relaxation parameter, or using multi-block grid system (Jameson, 1991).

2. Numerical Analysis

2.1 Governing equations

Axisymmetric, unsteady, compressible Navier-Stokes equation in general curvilinear coordinate system can be written in conservation law form as follows

$$\frac{1}{J}\frac{\partial q}{\partial \tau}+\frac{\partial}{\partial \xi}\frac{\xi_x}{J}f+1\frac{1}{\bar{y}}\frac{\partial}{\partial \xi}\frac{\xi_y}{J}g+\frac{\partial}{\partial \eta}\frac{\eta_x}{J}f+\frac{1}{\bar{y}}\frac{\partial}{\partial \eta}\frac{\eta_y}{J}g =\frac{\partial}{\partial \xi}\left(\frac{\xi_x}{J}f_v+\frac{\xi_y}{J}g_v\right)+\frac{\partial}{\partial \eta}\left(\frac{\eta_x}{J}f_v+\frac{\eta_y}{J}g_v\right) \tag{1}$$

Where q is conservative variable, f and g are inviscid fluxes as follows,

$$f=\begin{pmatrix}\rho u\\ \rho u^2+p\\ puv\\ (\rho e+p)u\end{pmatrix} \qquad g=\begin{pmatrix}ypv\\ y\rho vu\\ y(\rho v^2+p)\\ y(\rho e+p)v\end{pmatrix}$$

f_v and g_v are viscous fluxes which can be expressed in terms of primitive variables such as density, pressure, velocity and total energy.

The characteristic based upwind flux difference splitting method such as CSCM utilizes the properties of similarity transformation based on the conservative (q), the primitive ($\tilde{q}$) and the characteristic variables ($\tilde{\tilde{q}}$)

$$\begin{aligned}\partial_\xi F&=A\partial_\xi q=MT\Lambda T^{-1}M^{-1}\partial_\xi q\\ &=MT\Lambda T^{-1}\partial_\xi \tilde{q}=MA'\partial_\xi \tilde{q}\\ &=MT\Lambda\partial_\xi \tilde{\tilde{q}}\end{aligned} \tag{2}$$

where Λ is a diagonal matrix whose diagonal elements correspond to the eigenvalues. M matrix transforms primitive variables $\tilde{q}$ into conservative variables q. T^{-1} is a matrix which transforms primitive variables into characteristic variables. The inviscid flux ΔF can be divided into ΔF^+ and ΔF^- using diagonal truth function matrix $D^{\pm}$ and Equation 2 can be written as

$$\begin{aligned}\Delta F &= MTIT^{-1}A'\Delta\tilde{q}\\ &= MT(D^{+}+D^{-})\,T^{-1}A'\Delta\tilde{q}\\ &= \Delta F^{+}+\Delta F^{-}\end{aligned} \tag{3}$$

Using the relation $A'\Delta\tilde{q}=\tilde{M}^{-1}\Delta q$, the above equation can be rewritten as

$$\Delta F^{\pm}=MTD^{\pm}T^{-1}\tilde{M}^{-1}\Delta q=A^{\pm}\Delta q \tag{4}$$

Equation 4 satisfies the property 'U' of Roe and thus the fluxes are conserved.

The implicit finite difference equation can be discretized using one side differencing depending on the sign of eigenvalues of the jacobian matrices and are solved along ξ-direction and then η-direction successively.

CSCM (Conservative Supra Characteristic Method) upwind flux difference splitting methods based on Lombard et al.(1983) has been developed to study the intermittent flow (Oh et al. 2000) and the severe separated flow under adverse pressure gradient (Kim et al. 2004 ; Kim and Song, 2005).

2.2 Discretization

The governing equations are discretized by using finite difference method with second order accuracy in time (Oh et al., 2000) and space (Kim et al., 2004). Baldwin-Lomax (1978) algebraic turbulence model is used in this study. Second order time accurate dual time stepping method with inner iteration procedure for general grid point (i,j) can be written as follows

$$\left[\left(\frac{1}{J\Delta\tau}+\frac{1+\phi}{J\Delta t}\right)+A^{+}\nabla_{\xi}+A^{-}\Delta_{\xi}+B^{+}\nabla_{\eta}+B^{-}\Delta_{\eta}\right]\delta q^{n+1,k}=R^{n+1,k} \tag{5}$$

where n, $n+1$ indicate real time level, while k, $k+1$ represent pseudo time iteration level, Δ, ∇ are forward and backward space difference symbols, respectively. And residual $R^{n+1,k}$ can be written as

$$\begin{aligned}R^{n+1,k}=&-\frac{\phi\delta q^{n-1}}{J\Delta t}-\frac{(1+\phi)(q^{n+1,k}-q^{n})}{J\Delta t}\\ &-(A^{+}\nabla_{\xi}+A^{-}\Delta_{\xi}+B^{+}\nabla_{\eta}+B^{-}\Delta_{\eta})\,q^{n,k}\\ &-(A^{+}\nabla_{\xi}q_{i-1}+A^{-}\Delta_{\xi}q_{i}+B^{+}\nabla_{\eta}q_{j-1}+B^{-}\Delta_{\eta}q_{j})\end{aligned} \tag{6}$$

where the time accuracy coefficient ϕ was set to 0.5. $\Delta\tau$: real time, and Δt : pseudo time. A, B are Jacobian matrices. Jacobian matrices are computed once in physical time step and frozen for pseudo time subiterations. The second-order upwind flux difference splitting method using Fromm scheme (Kim and Song, 2005) with minmod limiter was used to discretize inviscid fluxes and viscous fluxes are centrally differenced. Implicit left hand side terms are approximately factored and subsequently diagonally dominant ADI method are used to keep the diagonal dominance of the resulting matrix system.

$$(-A^{+},E,A^{-})\,E\,(-B^{+},E,B^{-})\,\delta q^{n+1,k}=R^{n+1,k} \tag{7}$$

where $E=I+A^{+}-A^{-}+B^{+}-B^{-}$.

2.3 Boundary conditions and grid systems

Adiabatic wall condition was also used as thermal boundary condition for energy equation. And normal pressure gradient at the wall was assumed zero. Subsonic inlet flow conditions such as inflow direction, entropy, and total enthalpy were specified at the inlet. The exit static pressure was specified as atmospheric pressure (101.3 kPa). Along the nozzle centerline a symmetry condition was imposed. As wall boundary conditions, no-slip boundary conditions at the walls, i.e., $\mu_w=0$ and $v_w=0$. Two block grids system was used to simulate the nozzle flow-field. The viscous mesh placed a first grid point from the wall at y^{+} of unity. A stretching function was used to cluster grid points near the wall. Convergence of the solutions was considered to be achieved when the L^2 norm of the maximum residual reached 10^{-4}.

3. Results and Discussion

3.1 Unsteady flows over NACA0012 airfoil

Newly developed second-order time accurate dual time stepping Navier-Stokes code was used to verify the unsteady flow over a periodically oscillating NACA0012 airfoil as follows.

$$\alpha(t)=\alpha_0+\alpha_1\sin(M_{\infty}kt) \tag{8}$$

Following the AGARD Case 3 condition, Re$=4.8\times10^{6}$, $M_{\infty}=0.6$, $\alpha_0=4.86°$, $\alpha_1=2.44°$ and $k=0.162$ were used as test case conditions. Computed results were compared with Rumsey's experimental

results (1988). The physical time was nondimensionalized by $c/\sqrt{RT_\infty}$, where c, R, T_∞ were chord length, gas constant for air, and freestream temperature, respectively.

As shown in Figs. 1(a) and 1(b), current second-order time accurate dual time stepping method predicted better C_p values at the moment of ascending $\alpha=5.11°\uparrow$ and descending $\alpha=6.57°\downarrow$ when compared with first-order/second-order accurate time differencing method (Oh et al., 2000).

Figure 2 shows the lift coefficient variation (C_L) vs. angle of attack α over an oscillating period. Various time step sizes and number of sub iterations were exercised. It showed that the current dual time stepping method predicted much better lift coefficient than other time integration methods with different sub-iterations.

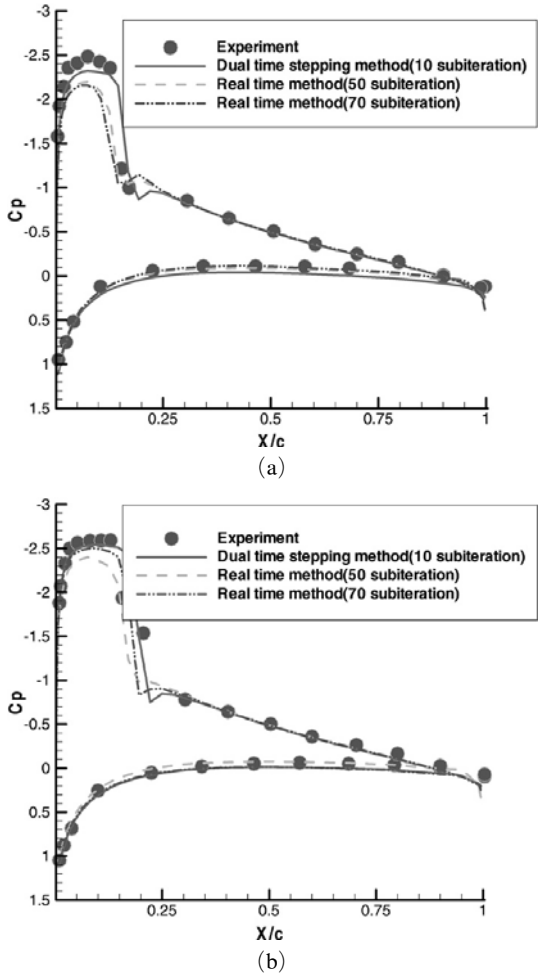

Fig. 1 Pressure coefficients for NACA0012 airfoil (a) $\alpha=5.11°\uparrow$, (b) $\alpha=6.57°\downarrow$

3.2 Steady flow analysis

Figure 3 shows a schematic drawing of main nozzle of an air-jet loom used in the computation. Major specifications of the main nozzle are inner diameter of needle, $d=2.8$ mm, acceleration tube length $L=270$ mm, and tube diameter $D=4.0$ mm. Flow passage in the main nozzle of an air-jet loom is divided into three regions. The first region includes an air tank, a two way-solenoid valve, air-jet main nozzle inlet, inclined flow passage, and the minimum cross-sectional area at the leading edge of the needle. Flow is accelerating in the convergent nozzle section. Sudden flow expansion in the backward facing step causes strong flow acceleration, and the accelerated flow pulls the weft into the acceleration tube in this second flow region. A massive flow separation right behind the backward facing step can be ob-

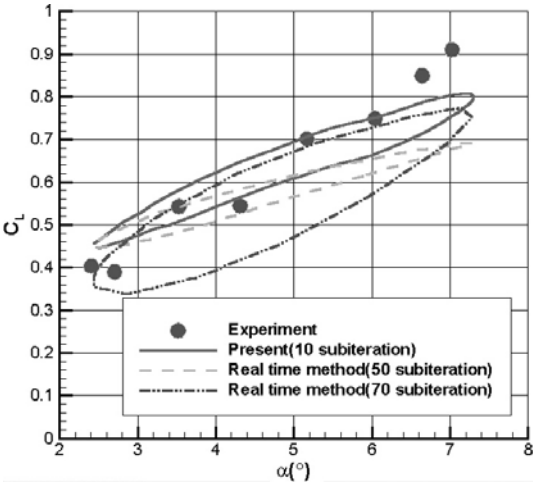

Fig. 2 Lift coefficients variation for oscillating NACA 0012 airfoil

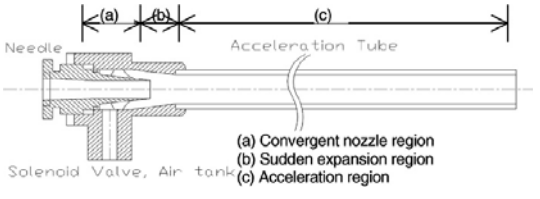

Fig. 3 Schematic diagram of main nozzle of air jet loom

served. Cross-sectional area is constant in the acceleration tube, and due to wall friction, boundary layer develops continuously inside the tube and eventually flow is accelerated to Mach 1 at tube exit in the third flow region, the "Fanno flow" region, as long as air tank pressure is sufficient.

Pulsating air from the solenoid valve is accelerated through a narrow stabilizer and flows into the main nozzle periodically. In this steady state study, we assume that air flows steadily into the nozzle even though it is pulsating. Computation begins at 13 mm upstream of nozzle throat where the flow is parallel to the axial direction. The actual main nozzle has a hollow needle (or yarn tube) in the middle for weft insertion, and co-axial surrounding flow passage is quite different from traditional nozzle. We computed the flow inside the nozzle by varying air tank pressure from 2 kg_f/cm^2~6 kg_f/cm^2.

Figure 4 shows the 154×70 H-type computational grid system generated by an elliptic PDE grid generator. We chose only the upper half of the centerline as computational domain due to axisymmetric flow assumption. We treated the hollow needle as a solid one to simplify the complex flow-field in a way similar to Mohamed and Salama (1986) and Oh et al.(2001). We assume the main nozzle system as an axisymmetric backward facing step. All the lengths are nondimensionalized by the radius of the acceleration tube (R=2.0 mm).

Figures 5(a)~5(e) show Mach number contours in the sudden expansion zone near the back-

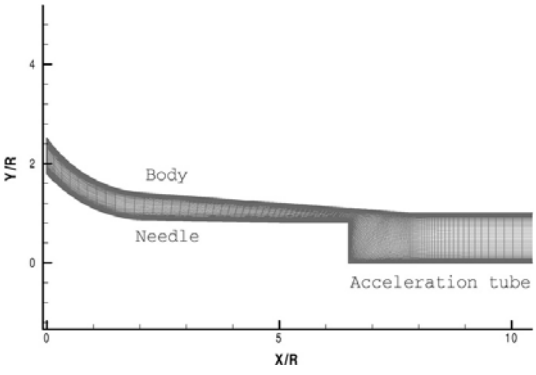

Fig. 4 Grid system in main nozzle

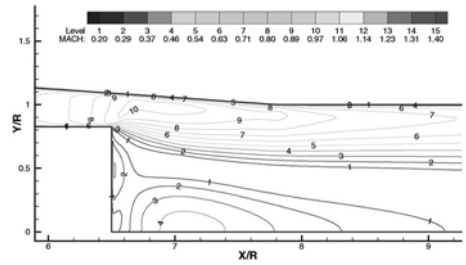

(a) 2 kg_f/cm^2

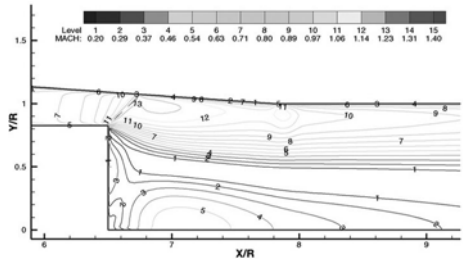

(b) 3 kg_f/cm^2

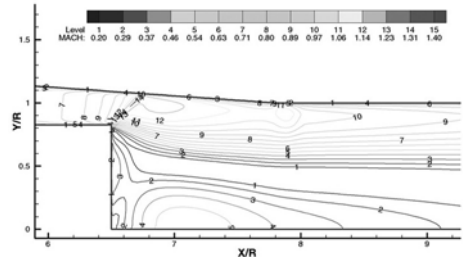

(c) 4 kg_f/cm^2

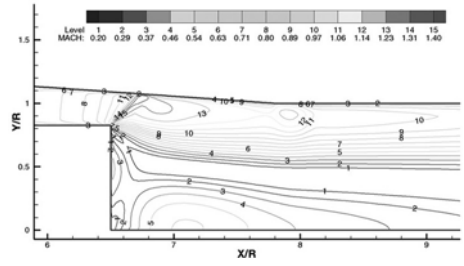

(d) 5 kg_f/cm^2

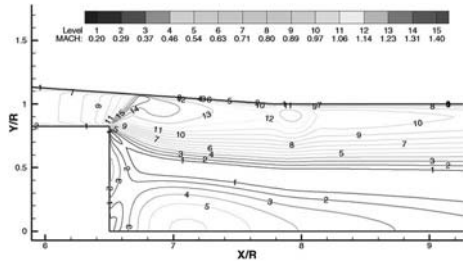

(e) 6 kg_f/cm^2

Fig. 5 Mach contours near the nozzle throat area at air tank pressure 2 kg_f/cm^2~6 kg_f/cm^2 respectively

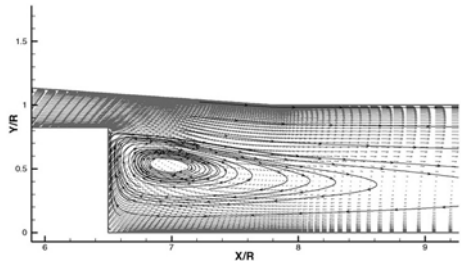

(a) 2 kg_f/cm^2

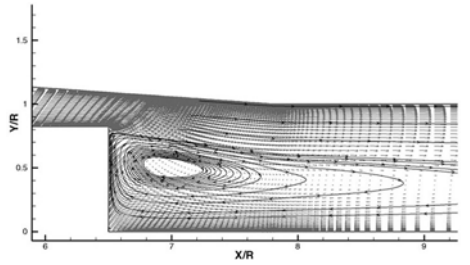

(b) 3 kg_f/cm^2

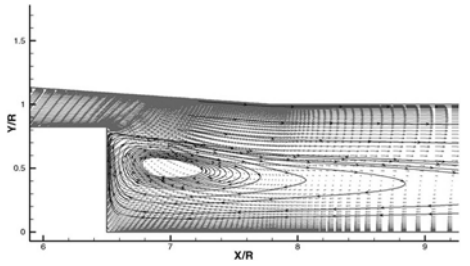

(c) 4 kg_f/cm^2

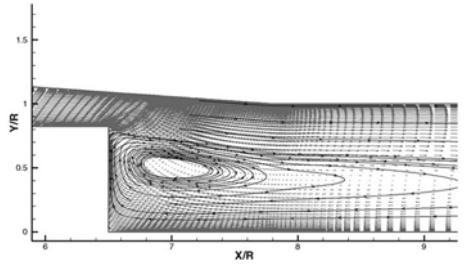

(d) 5 kg_f/cm^2

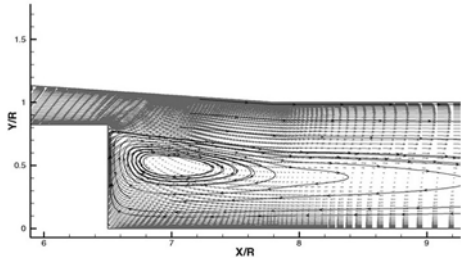

(e) 6 kg_f/cm^2

Fig. 6 Velocity vectors and streamline near the nozzle throat area at air tank pressure 2 kg_f/cm^2～6 kg_f/cm^2 respectively

ward facing step using Ishida and Okajima's test conditions (1994) (air tank pressures from 2 kg_f/cm^2～6 kg_f/cm^2). Due to the sudden expansion behind the nozzle throat, there are low supersonic flow regions at 2 and 3 kg_f/cm^2 air tank pressures; however, flow choking does not occur at the throat. At air tank pressures over 4 kg_f/cm^2 the flow reaches sonic ($M=1$) at the throat, and it shows similar flow patterns in Mach number contours near the backward facing step region.

Figures 6(a)～6(e) show velocity vectors and streamlines near the nozzle throat region. Decrease in flow velocity can be observed in reverse flow region near backward facing step due to flow separation and diffuser effect. The sizes of vortex behind the backward facing step show no big differences among each other as a whole.

In Fig. 7, the normalized free jet velocity at various x/d locations were plotted. All normalized data of free jet velocity profile were collapsed together showing self-similar velocity profile and compared with Gaussian function.

3.3 Unsteady flow analysis

The air tank stagnation pressure and temperature are set to 3.2 kg_f/cm^2 and 284.8 K, respectively, as test case condition. This condition is a little bit higher than that for steady flow in the previous section. The inflow through the solenoid

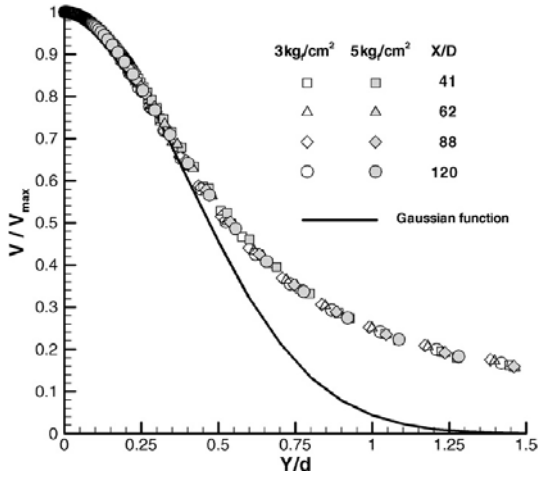

Fig. 7 Comparisons of few non-dimensional velocity profiles along path of free jet at 3 kg_f/cm^2 and 5 kg_f/cm^2 with Gaussian function

valve from the air tank was assumed as periodically pulsating flow. A period is 0.0531 second. Open-close time ratio of the solenoid valve is specified as 1 : 3 (refer to Fig. 8). Total enthalpy and pressure at inlet are set to constant during valve open time and wall boundary conditions are used to block flow influx through the inlet when closed.

As a result, Fig. 8 shows periodic total pressure variation from 1.58 kg_f/cm^2 to 3.2 kg_f/cm^2 at inlet region after about 200 periods (Fig. 9).

Figure 10 shows total pressure variations at nozzle inlet and end of backward facing step where real weft insertion takes place in AJL (Air Jet Loom) nozzle for three period time. Inlet total pressure were kept constant to a maximum value about 1/4 of period (≈0.013275 second).

Right after valve close at about 0.01548 second (or 0.29167 period), pressure at end of back ward facing step reaches to a maximum value (2.73855 kg_f/cm^2) from a minimum value (1.93 kg_f/cm^2) just before the valve close at about 0.01327 second (or 0.25/period). Meanwhile the minimum pressure was predicted to a larger value than a steady inlet value of 2.73855 kg_f/cm^2 for 3.0 kg_f/cm^2 air tank pressure. The weft release from the inlet hollow needle should begin at the moment of the minimum pressure at the end of backward facing step region for the best performance of air jet loom. In other words the weft needs to be released from the inlet of needle right after inlet valve close at the minimum pressure for better weft suction into the main nozzle.

Figure 11 shows the vortex change inside the main nozzle flow-field for a typical period. Peak pressure at the tip of backward facing step was observed when main flow from nozzle inlet passed through throat and suppressed large vortex toward centerline and back facing wall (0.292/period). The second peak pressure in the same location was observed when the expanded flow from the nozzle suppressed end of vortex (0.354/

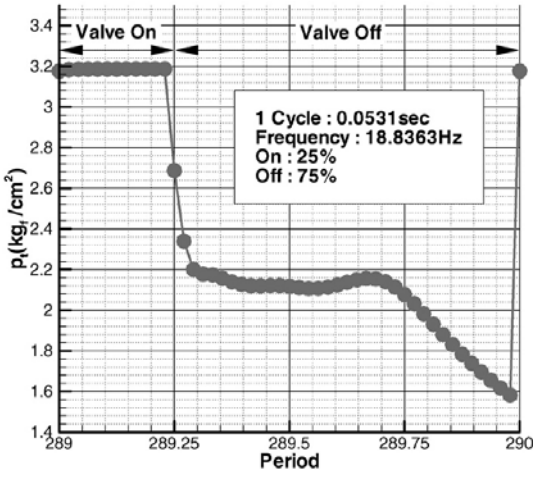

Fig. 8 Periodic inlet total pressure condition

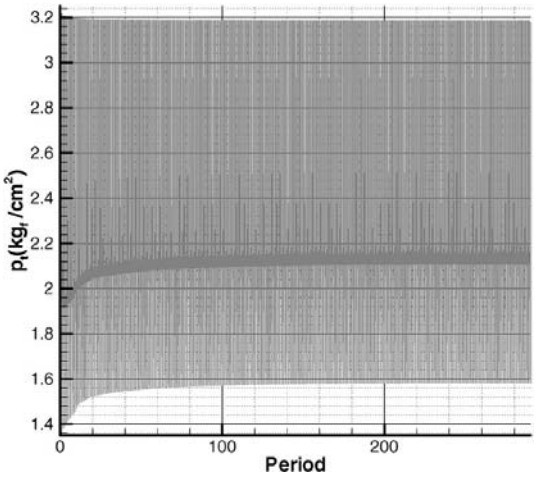

Fig. 9 Inlet total pressure variation along whole period

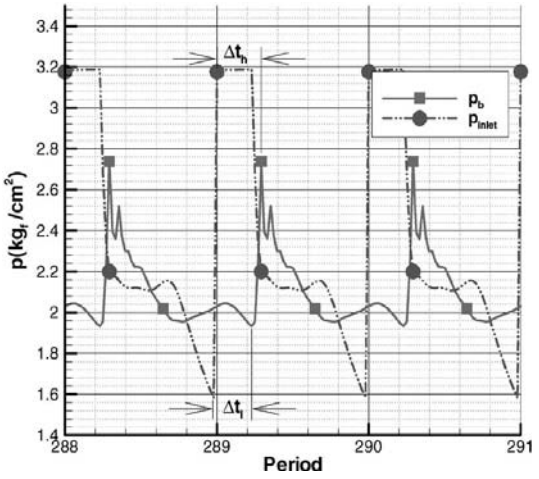

Fig. 10 Pressure variation comparison between inlet total pressure and backward facing step position

period). After the second peak pressure, size of the vortex enclosed by the main flow became larger as the main flow became weak, and thus pressure also decreased gradually.

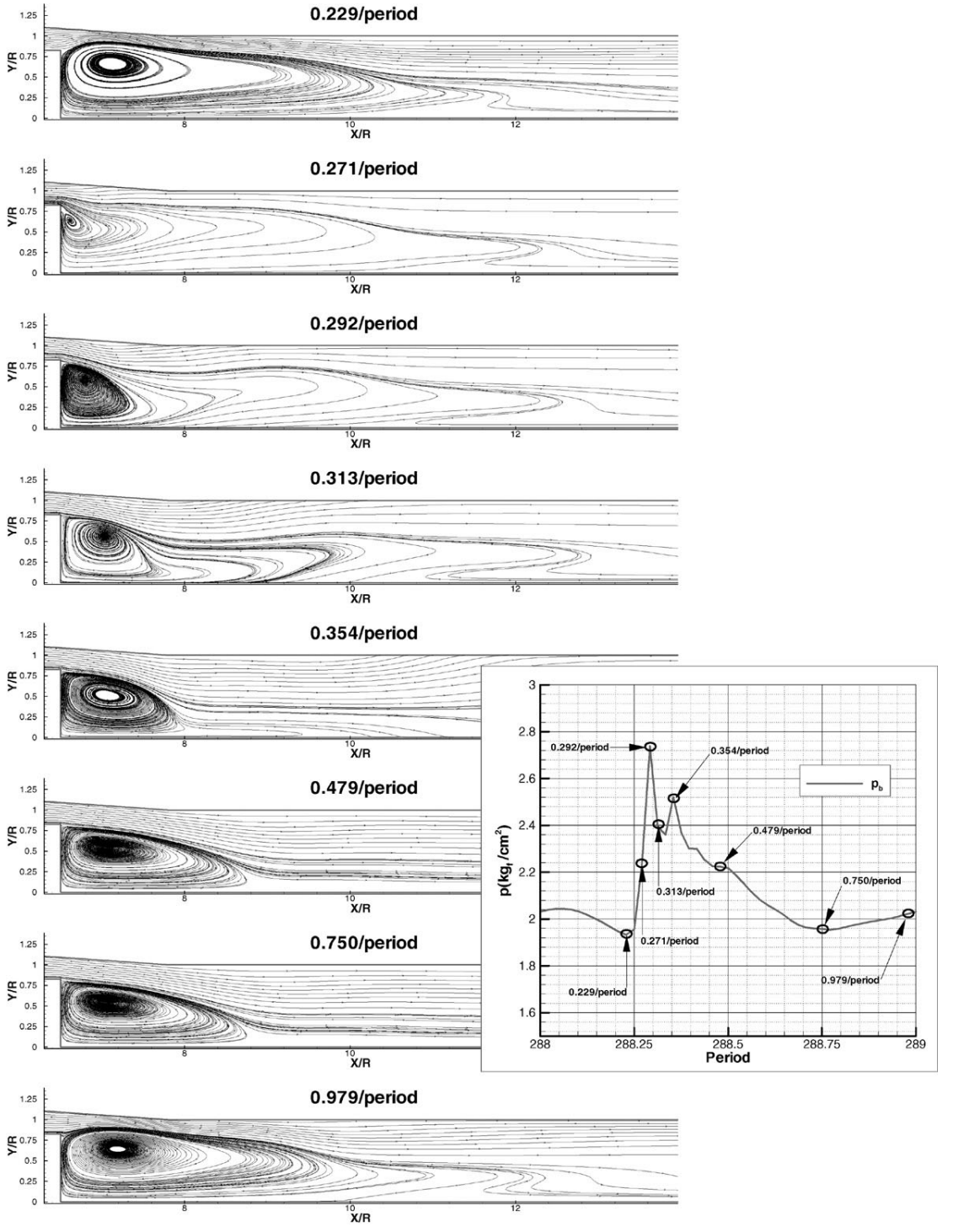

Fig. 11 Velocity vectors and streamline near the backward facing step nozzle for a typical period

Figure 12 shows Mach number and pressure contours near the backward facing step nozzle for a typical period. When the solenoid valve is opened, air is accelerated in the convergent nozzle region, pressure drops gradually and then rapidly to a minimum due to sudden flow expansion right after the backward facing step where cross-sectional area increases abruptly. Pressure is increased in recirculating flow region till entrance to acceleration tube showing adverse pressure gradient. This is chiefly due to flow acceleration to a maximum near throat region and sub-

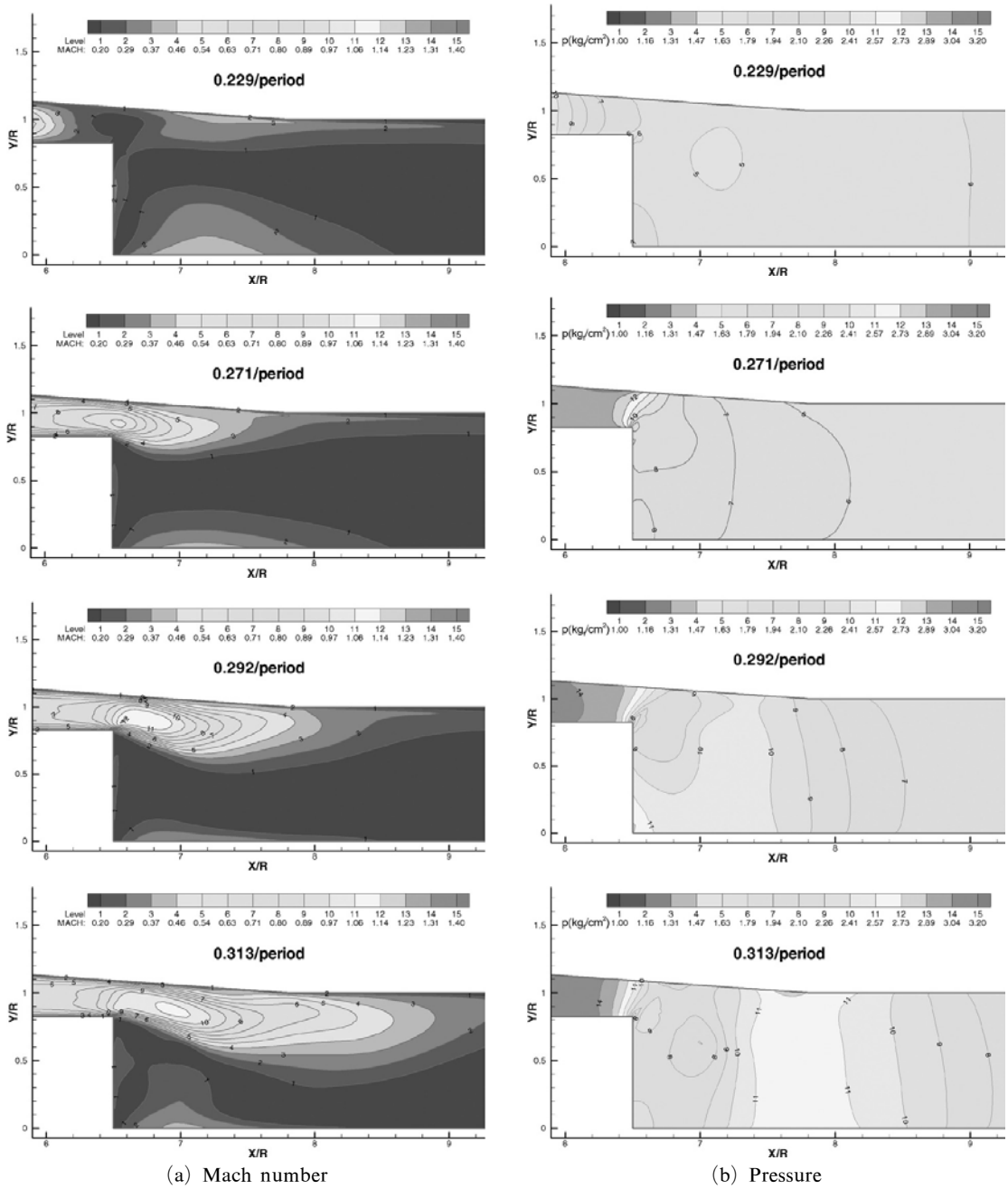

(a) Mach number (b) Pressure

Fig. 12 Mach number and pressure contours near the backward facing step for a typical period

sequent pressure recovery in the sudden expansion (divergent) zone because of diffuser effect. When the valve is closed at 0.25/period, the recirculating flow is developed due to flow separation occurance near nozzle throat, and the flow is accelerated and pressure near backward facing step drops further.

Figure 13 shows pressure distribution along the centerline. Due to main flow over vortex the peak pressure was transported downstream after 0.313/period.

The x-momentum (ρu) along the centerline is

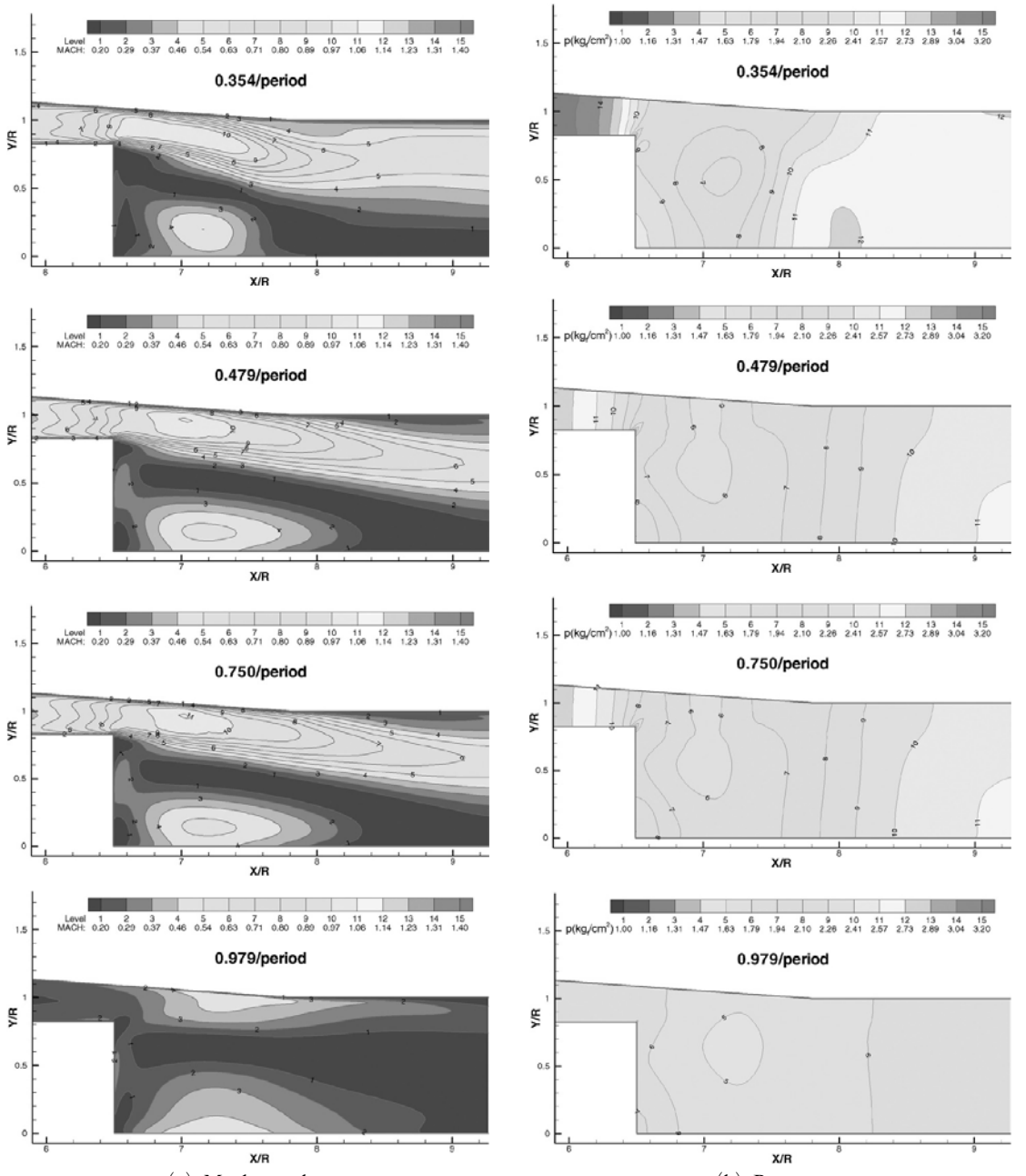

(a) Mach number (b) Pressure

Fig. 12 Mach number and pressure contours near the backward facing step for a typical period

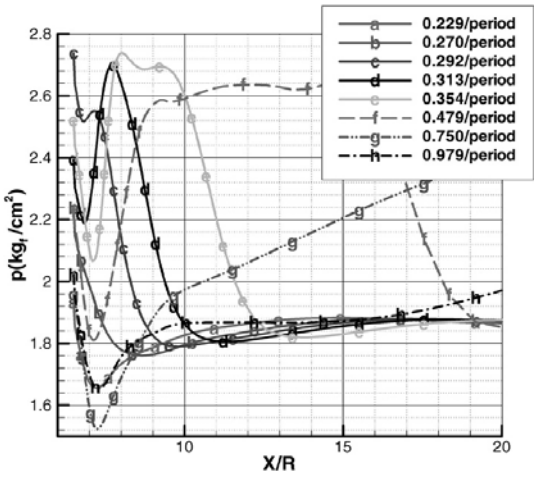

Fig. 13 Pressure distributions along the centerline at each period

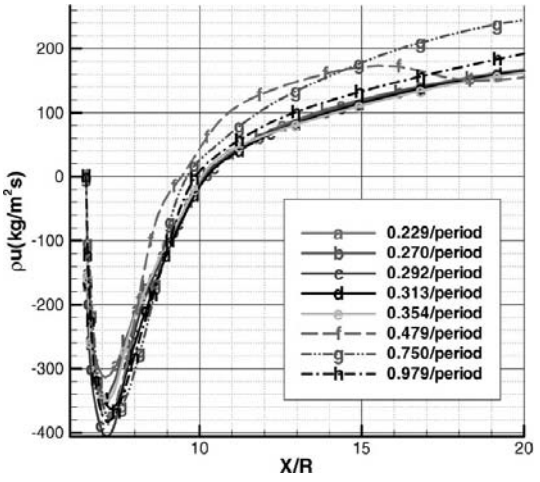

Fig. 14 Momentum distributions along the centerline at each period

shown in Fig. 14. Due to vortex recirculating flow extends toward about $x/R \approx 10$; however, momentum difference was relatively small when compared to pressure change.

4. Conclusions

The steady and unsteady transonic/supersonic flows in an axisymmetric backward facing step shape main nozzle of an air jet loom have been analyzed by using upwind flux difference splitting Navier-Stokes method. At air tank pressures of 4 kg_f/cm^2 or higher choking phenomena occurred at the nozzle throat and the exit of the acceleration tube. Mach number contour distribution near the main nozzle throat and backward facing step was similar to each other at air tank pressures of 4 kg_f/cm^2 or higher. In unsteady flow analysis, periodic flow pattern was observed in backward facing step region. When the solenoid valve is opened, pressure is increased in recirculating flow region till entrance to acceleration tube showing adverse pressure gradient due to flow acceleration to a maximum near throat region and subsequent pressure recovery in the sudden expansion zone. When the valve is closed, the recirculating flow is developed due to flow separation occurrence near nozzle throat, and the flow is accelerated and pressure near backward facing step drops further.

Acknowledgments

This work was partially supported by 2006 Yeungnam University 2nd stage BK21 project.

References

Baldwin, B. S. and Lomax, H., 1978, "Thin Layer Approximation and Algebraic Model for Separated Turbulent Flows," AIAA paper 78-257.

Chow, L. J. and Pulliam, T. H., 1984, "A General Perturbation Approach for Computational Fluid Dynamics," *AIAA J.*, Vol. 22, No. 12, pp. 1748~1754.

Duxbury, V. and Lord, P.R., 1959, "A Study of Some Factors Involved in Pneumatic Weft Propulsion," *Journal of Textile Institute*, Vol. 50, No. 10.

Ishida, M. and Okajima, A., 1994, "Flow Characteristic of the Main Nozzle in an Air-Jet Loom," *Textile Research Journal*, Vol. 64, No. 1, pp. 10~20.

Jameson, A., 1991, "Time Dependent Calculations Using Multigrid with Application to Unsteady Flows Past Airfoils and Wings," AIAA Paper 91-1596.

Jorgenson, P. C. E. and Chima, R. V., 1989,

"Explicit Runge-Kutta Method for Unsteady Rotor/Stator Interaction," *AIAA Journal*, Vol. 27, No. 6, pp. 743～749.

Kim, S. D. and Song, D. J., 2005, "Modified Shear-Stress Transport Turbulence Model for Supersonic Flows," *Journal of Aircraft*, Vol. 42, No. 5, pp. 1118～1125.

Kim, S. D., Kwon, C. O. and Song, D. J., 2004, "Comparison of Turbulence Models in Shock-Wave/Boundary-Layer Interaction," *KSME International Journal*, Vol. 18, No. 1, pp. 153～166.

Lombard, C. K., Bardina, J., Venkatapathy, E. and Oliger, J., 1983, "Multi-dimensional formulation of CSCM-An Upwind Flux Difference Eigenvector Split Method for the Compressible Navier-Stokes Equations," AIAA-83-1859cp.

Lyuboviskii, V. P., 1966, "Analysis of the Pulsed Air Flow on the P-105 Loom," *Technology of Textile Industry. USSR*, No. 6, pp. 114.

Mohamed, M. H. and Salama, M., 1986, "Mechanics of a Single Nozzle Air-Jet Filling Insertion System," *Part 1, Textile Research Journal*, Vol. 56, No. 11.

Oh, T. H., Kim, S. D. and Song, D. J., 2000, "Unsteady Transonic Flow Analysis Over an Oscillating Airfoil," *KSAS Journal*, Vol. 28, No. 2, pp. 10～17.

Oh, T. H., Kim, S. D. and Song, D. J., 2001, "A Numerical Analysis of Transonic/Supersonic Flows in the Axisymmetric Main Nozzle of an Air-Jet Loom," *Textile Research Journal*, Vol. 71, No. 9, pp. 783～790.

Rumsey, C. L. and Anderson W. K., 1988, "Some Numerical and Physical Aspects of Unsteady Navier-Stokes Computations Over Airfoils Using Dynamic Meshes," AIAA-88-0329.

Uno, M. and Ishida, T., 1960, "A study on Air Jet Looms (in Japanese)," *Journal of Textile Machine Society*, Vol. 13, No. 9.